

# Structure Learning of Quantum Embeddings

Massimiliano Incudini<sup>1\*</sup>, Francesco Martini<sup>1</sup>  
and Alessandra Di Pierro<sup>1</sup>

<sup>1\*</sup>Dipartimento di Informatica, Università di Verona, Verona,  
34137, Italy.

\*Corresponding author(s). E-mail(s):  
[massimiliano.incudini@univr.it](mailto:massimiliano.incudini@univr.it);

## Abstract

The representation of data is of paramount importance for machine learning methods. Kernel methods are used to enrich the feature representation, allowing better generalization. Quantum kernels implement efficiently complex transformation encoding classical data in the Hilbert space of a quantum system, resulting in even exponential speedup. However, we need prior knowledge of the data to choose an appropriate parametric quantum circuit that can be used as quantum embedding. We propose an algorithm that automatically selects the best quantum embedding through a combinatorial optimization procedure that modifies the structure of the circuit, changing the generators of the gates, their angles (which depend on the data points), and the qubits on which the various gates act. Since combinatorial optimization is computationally expensive, we have introduced a criterion based on the exponential concentration of kernel matrix coefficients around the mean to immediately discard an arbitrarily large portion of solutions that are believed to perform poorly. Contrary to the gradient-based optimization (e.g. trainable quantum kernels), our approach is not affected by the barren plateau by construction. We have used both artificial and real-world datasets to demonstrate the increased performance of our approach with respect to randomly generated PQC. We have also compared the effect of different optimization algorithms, including greedy local search, simulated annealing, and genetic algorithms, showing that the algorithm choice largely affects the result.

**Keywords:** Quantum Kernel, Quantum Embedding, Quantum Machine Learning, Quantum Computing, Quantum Optimization, Kernel Optimization, Simulated Annealing, Genetic Algorithms

# 1 Introduction

Quantum machine learning [1] aims to exploit the properties of quantum computation to improve the performances of machine learning models in terms of speed or accuracy. Early works have aimed to find strong, rigorous speedup based on the HHL algorithm for matrix inversion [2], a building block for many algorithms such as the quantum SVM [3] and quantum PCA [4]; or to find topological properties of data [5]. These approaches require reliable quantum hardware, severe assumptions on the data (e.g. sparsity), [6] and the use of QRAM [7], a hypothetical hardware device that allows efficient access to a quantum state. Recent works have been focused on NISQ-ready algorithms [8], i.e. algorithms that can be run on noisy quantum devices with a limited number of qubits. The most notable techniques are the variational quantum algorithms [9] such as VQE [10] and QAOA [11, 12] exploiting both quantum and classical hardware to solve material-related and combinatorial optimization problems, and Quantum Neural Networks [13] to solve supervised learning tasks. Among these techniques, quantum kernels [14] are one of the most promising.

Quantum embedding and quantum kernels are powerful data analysis techniques that allow us to define non-linear predictors through the encoding of classical data into a quantum system. The use of (classical) kernel methods in machine learning [15, 16] has found applications in many field of science including biology [17], chemistry [18] and physics [19]. Most kernel methods algorithms such as Ridge Regression and kernel PCA are based on convex optimization and thus are efficiently solvable on classical hardware. Kernel methods use positive definite, symmetric functions to encode data points into a Reproducible Kernel Hilbert Space (RKHS). Quantum kernel naturally arises from the similarity between the RKHS and the Hilbert space of the quantum system: each parametric quantum transformation that encodes the data within a quantum state is an embedding function [20], and taking the inner product between quantum states encoding the data points (eg. through the swap test [21] or the fidelity measure) implements a kernel function.

Quantum kernels are a well-studied algorithmic technique. The use of quantum kernel can lead to an exponential speedup over classical machine learning algorithms on artificially generated tasks [22]. They have been used to efficiently classify group-structured data [23] and to predict properties of quantum systems [24]. In [24], the concept of *projected* or *biased* quantum kernel is introduced, which first exploits the high-dimensional Hilbert space of the quantum system to perform complex transformations, then projects the states into a low-dimensional subspace to mitigate the curse of dimensionality. The approach requires prior knowledge to choose a favorable projection. In [25], expressible quantum transformations are introduced, which are able to spread vectors all over the Hilbert space, and are shown to lead to machine learning models that can learn no function. Almost-constant transformations are the only ones capable to generalize. In [26], it is suggested that a good generalization is obtained by limiting the angle of parametric rotational gates using a tunable hyper-parameter called bandwidth. The problem of expressibility of quantum transformations [27] is closely related to the barren plateau [28] in quantum

neural networks, in which the variance of the gradient vanishes exponentially in the system size, preventing learning. An effect similar to the barren plateau happens in quantum kernels when the non-diagonal coefficients of the kernel matrix are concentrated around a single value [29], with variance decreasing exponentially in the system size. It has been shown in [30] that the choice of generators of the quantum transformations greatly affects the expressibility of the model.

In this work, we deal with the problem of deciding the structure of quantum transformations in the form of the parametric quantum circuit (PQC, [31]) without any prior knowledge of the problem data to guide the choice. The lack of prior knowledge is a common situation for most real-world datasets. The works in [23, 32] propose trainable quantum embeddings, i.e. PQC parameterized both by the data point features and some trainable angle, which can be learned through gradient-descent based algorithm to minimize some loss function. Such an approach still requires prior knowledge to decide the structure of the transformation, and the barren plateau might prevent the optimization. [33] has pioneered the use of genetic algorithms to place random gates automatically. However, the latter approach has an expensive optimization procedure that penalizes non-local gates, leading to circuits having only local operation and being therefore classically simulatable. Another work [34] has improved the optimization by penalizing the circuit length. A similar approach has been proposed in [35] by using variational quantum algorithms.

In our work, we model the problem of choosing the best structure for the PQC of the quantum kernel as a combinatorial optimization problem. The structure of the circuit has a fixed number of gates, avoiding the need for a circuit length penalty. The structure of the circuit can be optimized using any meta-heuristic such as greedy local search, simulated annealing, and genetic algorithms. The principal objects of our optimization are the generators of the gates. As shown in [30], these generators largely influence the expressibility of the circuit. Any combinatorial optimization process is computationally expensive. To lower this computational cost, we have introduced an efficient policy to evaluate candidate solutions, based on the exponential concentrations of inner products around the average value [29]. In contrast to the gradient-descent-based approach, our optimization does not suffer from the barren plateau problem by construction and leads to solutions that are not affected by unfavorable numerical properties. We have tested our approach on several real-world and artificial datasets. In particular, we have used greedy local search, simulated annealing, and genetic algorithms to optimize our PQC. Finally, we have compared our results with those obtained with other stochastic-based techniques for designing quantum embedding.

## 2 Background

Consider the regression setting where we are trying to learn the function  $f$  such that  $Y = f(X) + \epsilon$ , where random variable  $X$  having domain  $\Omega \subset \mathbb{R}^d$  and probability distribution  $\mu$ , and  $\epsilon$  represents noise sampled from a Gaussian

distribution having zero mean. Consider the set of observations  $\{(x^{(i)}, y^{(i)})\}_{i=1}^n$  where  $x^{(i)}$  is i.i.d. sampled from  $\mu$  and  $y^{(i)} = f(x^{(i)}) + \epsilon$ .

## 2.1 Kernels Methods, and their Spectral and Probabilistic Properties

Kernel methods [15] generalizes the notion of similarity between data samples, allowing the definition of predictors that are nonlinear in  $\Omega$ . A Mercer kernel  $k : \Omega \times \Omega \rightarrow \mathbb{R}$  is positive definite and symmetric. Kernel methods can be used to enhance most similarity-based algorithms: Kernel Ridge Regression [36] (KRR) is a generalization of the linear regressor, in the form

$$\hat{f}(x) = \sum_{i=1}^n \alpha_i k(x^{(i)}, x) \quad \alpha_i = \sum_{j=1}^n ((k(x^{(i)}, x^{(j)}) - \lambda))^{-1} y_j \quad (1)$$

where  $\lambda > 0$  is the regularization term that penalizes higher norm solutions, avoiding overfitting of noise. The predictor minimizes the mean square error. The Support Vector Machine [37] (SVM) defines a similar predictor with lower memory consumption. Kernel Principal Component Analysis [38] (K-PCA) finds the directions that best fit the data in  $\mathcal{H}$ . The similarity between data points is completely specified by the kernel matrix  $K = [k(x^{(i)}, x^{(j)})]_{i,j=1}^n$ , which can be rescaled such that  $\text{Tr}[K] = 1$ . The Mercer kernel  $k$  allows the spectral decomposition

$$k(x, x') = \sum_{i=1}^{\infty} \gamma_i \phi_i(x) \phi_i(x') \quad (2)$$

where  $(\gamma_i)_{i>0}$  is a sequence of non-increasing numbers and  $(\phi_i)_{i>0}$  are orthonormal functions. These are the eigenvalues and eigenfunctions of the integral operator

$$T[g] = x \mapsto \int_{\Omega} k(x, x') g(x') d\mu(x'). \quad (3)$$

The eigenvalues of a finite kernel matrix  $K$  approximate  $(\gamma_i)_{i>0}$  as  $n \rightarrow \infty$  [x]. The study of eigenvalues is of paramount importance: for example, [38] have used to identify the principal components, and [39] to define lower bounds to the approximation error between  $f$  and  $\hat{f}$ , [40] relates it to the concentration of random kernel matrices around their mean. Note that if the non-diagonal values of a single kernel matrix are highly concentrated around its mean, the learning is made difficult and requires higher precision to distinguish the distance between different pairs of points [29]. [41] quantify the quality of learning  $f$  with the kernel  $k$  using the target-kernel alignment

$$A(k, g) = \frac{\langle k, g^{\otimes 2} \rangle}{\|k\| \|g\|} \quad (4)$$

with  $0 \leq A(k, g) \leq 1$ , the higher the better, and can be related to the eigenvalue distribution too. It has been used to learn kernel functions themselves [42].

## 2.2 Parametric Quantum Circuits

Consider the Hilbert space  $\mathcal{H} = (\mathbb{C}^2)^{\otimes n}$  and the group of unitary operators  $\mathcal{U}$  acting on  $\mathcal{H}$ . A parametric quantum circuit (PQC) [31] is an family of unitary transformations  $U : [0, 2\pi]^{LK} \rightarrow \mathcal{U}$  in the form

$$U(\theta) = \prod_{\ell=1}^L \prod_{k=1}^K W_k \exp(-i\theta_{\ell k} H_k) V_k \quad (5)$$

where  $W_j, V_j \in \mathcal{U}$  are arbitrary, non-parametric unitaries and  $H_j$  is the generator, i.e. traceless Hermitian matrix, which can be expressed as the sum of products of Pauli matrices. The parameters  $\theta$  can be optimized to minimize a cost function  $C(\theta) = \langle 0|U(\theta)OU^\dagger(\theta)|0\rangle$ . The optimization is possible if we do not encounter the barren plateau phenomena [28]:  $\nabla_\theta C$  approaches zero exponentially fast with respect to  $n$ , resulting in the lack of a gradient direction for the training.

The expressibility of a PQC [43, 44] is the ability of the PQC to generate pure states exploring all  $\mathcal{H}$ . The expressibility can be quantified by comparing the distribution of states  $\mathcal{E}$  generated by  $U(\theta)$  and the uniform distribution of states (Haar random states) using the formula

$$A = \int_{\text{Haar}} (|\phi\rangle\langle\phi|)^{\otimes t} d\phi - \int_{\mathcal{E}} (|\psi\rangle\langle\psi|)^{\otimes t} d\psi. \quad (6)$$

If  $\|A\|_\infty \leq \varepsilon$  then  $U$  is an  $\varepsilon$ -approximate  $t$ -design. As  $t$  grows, the distribution of state approximates better than the Haar distribution. [27] has defined an upper bound on the gradient magnitude given the expressibility of a PQC: if the group of unitaries generated by  $U(\theta)$  forms a 2-design, then the variance of  $\nabla_\theta C$  vanishes exponentially fast in  $n$ . The lack of expressibility does not guarantee a large gradient magnitude: global cost function [45] and noise [46] contribute to the appearance of the barren plateau.

The expressibility of a PQC  $U(\theta)$  is strongly related to the controllability problem in Quantum Optimal Control:  $U(x)$  is (pure state) controllable if  $\forall |\phi\rangle, |\psi\rangle$  exists  $\bar{\theta}$  such that  $|\phi\rangle = U(\bar{\theta})|\psi\rangle$  [47]. Given the set of generators  $\{H_k\}_{k=1}^K$  of  $U(\theta)$ , we can define the Dynamical Lie Algebra (DLA) as the span of  $\{iH_k\}$  under the operation of commutation. The system is controllable, thus maximally expressible, if the DLA is full rank. In particular, a DLA polynomially sized in  $n$  may lead to trainable circuits while exponentially sized DLA will not [30, 48].

## 2.3 Quantum Kernels

Quantum kernel methods [14] are obtained by encoding a couple of data points  $x, x'$  within the Hilbert space of the quantum system of  $n$  qubits using a unitary

encoding  $U : \Omega \rightarrow \mathcal{U}$  in the form of Equation 5 then taking the inner product. The latter calculation can be efficiently estimated with the fidelity measure:

$$k(x, x') = \langle 0|U(x)\sigma_z^{\otimes n}U^\dagger(x')|0\rangle \quad (7)$$

or alternatively, with the SWAP test [21]. If  $U$  is not classically simulable there is the possibility of a quantum advantage, which has been already proven for highly artificial tasks [22, 25].

The exponential dimensionality of  $\mathcal{H}$  may deteriorate the fidelity-based quantum kernel due to the curse of dimensionality: the inner product between two (random) vectors is expected to reach zero as  $n$  grows. [24] have introduced projected or biased kernel:

$$\phi(x) = \langle 0|U(x)OU^\dagger(x)|0\rangle \quad k(x, x') = \exp(-\gamma\|\phi(x) - \phi(x')\|) \quad (8)$$

where  $\lambda > 0$ , which projects the quantum state toward a lower-dimensionality subspace using the observable  $O$ , e.g. a local  $\sigma_z$  measurement of  $k \leq n$  qubits. Biased kernels have been used to learn the prediction of a quantum system from experimental data [24].

[25] have studied the spectral properties of quantum kernels, and proven that learning is feasible with fidelity-based quantum kernels only if  $U$  is almost constant, i.e. don't exploit the whole (exponentially sized) Hilbert space. This aspect seems to be strongly related to the expressibility characteristic leading to the barren plateau in PQC. [25] have suggested that even biased kernels are problematic to use in practice if we have no assumptions suggesting to us which observable  $O$  projects the data onto a subspace of  $\mathcal{H}$  that well represents our points. [25, 29] have shown that expressible unitaries lead to kernel matrices whose non-diagonal elements are exponentially concentrated around their mean, requiring an exponential amount of measurements to distinguish the kernel value of different pairs of points. Other sources of concentrations are noise and high entanglement [29].

Finally, [26] has shown that the rescaling of input by a constant (bandwidth) can improve the generalization error of quantum kernels, therefore is an important hyperparameter to optimize.

### 3 Learning the structure of quantum circuits

As stated in [23], if we have enough assumptions to decide the set of generators a priori, i.e. fixing the structure of the PQC, we can effectively optimize some parameters using target-kernel alignment techniques. However, in many problems we lack such assumptions and struggle to fix an effective structure for the PQC; this forces us to select an expressible form that is difficult to train.

Here we introduce an approach where the object of the optimisation is the structure of the generators rather than the circuit itself. More precisely, we define a combinatorial optimization problem whose objective function is a scheme for PQC where each gate corresponds to a variable ranging in the set

of allowed generators. We assume that input  $x$  has already undergone a pre-processing that has extended it with nonlinear classical pre-calculated features (e.g.  $x_{d+1} = x_k \cdot x_{k'}$  for some  $k, k' < n$  as in [14]) and that data are rescaled according to a bandwidth [26].

### 3.1 Structure of the quantum embedding

We propose a rigid structure for a PQC composed of  $L$  repeated layers of  $2n$  gates, where  $n$  corresponds also to the number of features. In this structure, depicted in Figure 1, each layer is composed of a column of single-qubits gates followed by a column of two-qubits gates acting on (circularly) adjacent qubits. Each gate is associated with a generator in  $P = \{\mathbb{I}_2, \sigma_x, \sigma_y, \sigma_z\}$  (for single-qubit gates) or  $P^{\otimes 2}$  (for two-qubits gates), and an angle corresponds to one of the components of  $x$ . The PQC can be described by a  $2 \times 2Ln$  matrix where each column corresponds to a quantum gate in a fixed position indicated by the first component of the column (generator), and the second component (the angle).

Alternatively, a more flexible structure can be used: we can set  $m$  to the number of (local or non-local) gates and let the optimization process decide which operation to perform on which qubit. This formulation comes at the expenses of searching in a much larger space of candidate solutions. In this case, the PQC can be described by a  $4 \times m$  matrix, where each column corresponds to a quantum gate in an arbitrary position: the two components correspond to the ones in the rigid structure, and the third and fourth components are the pair of qubits, which the gate acts on (0 to  $n - 1$ ). Such structure is shown in Figure 2 and allows for short, effective circuits at the expenses of having a larger discrete space of candidate solutions. This structure shares some similarities with the one proposed by [33], except that, contrary to the latter, in our approach the number of gates is fixed, thus avoiding the need for a penalty due to unreasonably long circuits.

For both structures in Figure 1 and Figure 2, the initialization consists of finding an initial value for the matrix representing the PQC. Initialization can be deterministic, by choosing the zero matrices, or stochastic, by selecting the values randomly. Each row has its own domain: the first row contains elements of  $P \cup P^{\otimes 2}$ , and the second row contains features of  $x \in \mathbb{R}^n$ . For the flexible structure, the third and fourth rows range in the list of qubits (which we have fixed to  $n$  as the number of features). The pseudocode describing the construction of this family of PQC is shown in Figure B.

### 3.2 Optimization

The optimization phase has to select the best matrix (i.e. PQC) according to a certain cost function. Since the space of solution is exponential in the number of variables, exhaustive search is not a good option for finding a global optimum. We instead rely on deterministic or stochastic meta-heuristics, which give us no guarantees about the quality of the solution but generally lead to satisfactory solutions.

We have selected three well-known approaches: a greedy (local) search, the simulated annealing algorithm [49] and the genetic optimization algorithm [50].

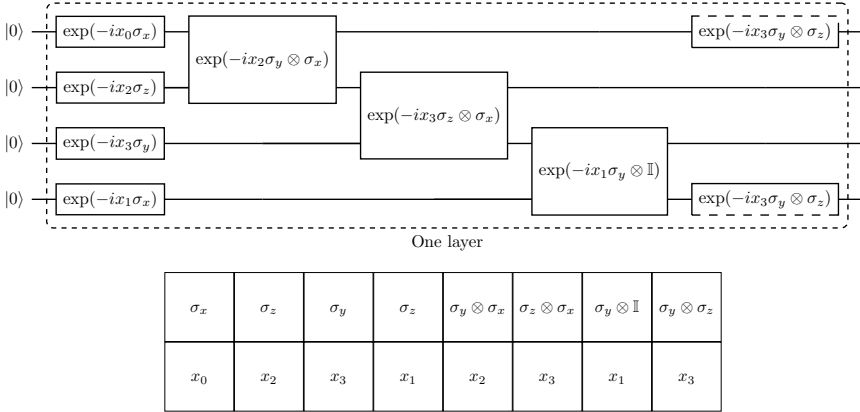


**Fig. 1:** An instance of a circuit having  $n = 4$  qubits and  $L = 1$  layers. The embedding can be represented by the  $2 \times 2Ln$  matrix below the circuit. There is a bijection between PQC and its matrix representation. Each column corresponds to a (parameterized) gate at a fixed position: the first  $n$  gates of each layer are 1-local, and the last  $n$  are 2-local. The first component of the column is the generator ranges in  $P^{\otimes 2}$  (if the operation is 1-local, the second Pauli matrix is ignored) while the second component is one of the features of  $x$  (assumes  $x \in \mathbb{R}^n$ ).

Such techniques are discussed in Appendix A. Heuristics for combinatorial optimization is an active field of research and many more approaches exist in the literature, some of the most notable being Taboo Search [51], Graph Neural Networks [52] and Reinforcement-Learning-based techniques [53]. It is important to notice that our approach gives a general scheme for constructing kernels, which can be used with any optimization algorithm.

### 3.3 Cost function evaluation

To evaluate the quality of solutions we utilize a cost function that minimizes the expressibility and maximizes the accuracy.

Earlier approaches [33, 34] penalize the length of the circuit or the number of CNOT gates; however, this does not necessarily guarantee that the circuit becomes non-maximally expressive [30].

The expressibility can be quantified in different ways as discussed in Section 2.2. Instead of expressibility, we use another quality based on an estimate of the concentration around the mean [29]. We use the quantum kernel to calculate a small, constant number of similarities between randomly chosen pairs of data points: if the variance of the values is below an arbitrary threshold, the PQC is immediately discarded.

The accuracy can be estimated by first training an SVM (whose kernel matrix is the result of our PQC) with respect to a training set, and then calculating the mean square error with respect to a validation set. Note that

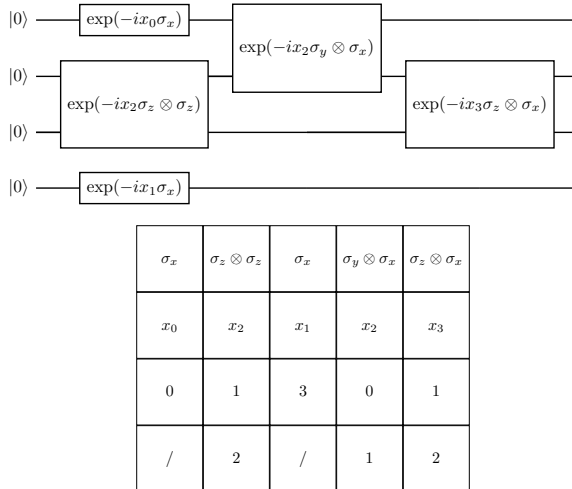


**Fig. 2:** An instance of a circuit having  $n = 4$  qubits and  $m = 5$  gates. The embedding can be represented by the  $4 \times m$  matrix below the circuit. Each column corresponds to a 1-local or 2-local qubits (parameterized) gate at an arbitrary position: the first component is the generator in  $P^{\otimes 2}$ , the second one is the feature of  $x$  to be used as a rotational parameter, and the third and fourth are the qubits in which the transformation will act to (the fourth component may be ignored if the generator acts non-trivially on a single qubit).

the target-kernel alignment can be used as a proxy for the empirical (training) error but cannot be straightforwardly used for the generalization error.

Calculating the expressibility cost as concentration around the mean is much faster than calculating the accuracy cost, which requires the computation of the kernel matrix. Therefore, it is convenient that the overall cost function is *not* a linear combination of the two terms, which would force the calculation of both terms. Instead, we first calculate the expressibility; if this is above a certain threshold, we immediately return cost  $\infty$  without calculating the accuracy. Otherwise, the cost is directly the (estimated) generalization error. If the expressibility is large enough to discard most solutions, the overall optimization phase is quite fast.

## 4 Application to artificial and real-world problems

To test the efficacy of our formulation, we have tested our approach on both artificially generated and real-world regression problems. We have compared the quantum kernel generated using random PQC compared with the combinatorial quantum kernel (optimized using greedy, simulated annealing, and genetic algorithms). The implementation details and the instructions to download the code and reproduce the experiments are detailed in Appendix C.

## 4.1 Datasets

We have generated three artificial dataset: the first dataset is generated by sampling  $\sin^2(x)$ , the second one by sampling the step function  $f(x) = (\text{sign}(x)+1)/2$ , the third one by sampling the Meyer Wavelet  $\psi$  function [54]. Each artificial dataset has 100 elements  $\{(x^{(i)}, y^{(i)})\}_{i=1}^{100}$  with  $x^{(i)} \in \mathbb{R}^2$ ,  $x_0^{(i)} = x_1^{(i)}$  uniformly sampled from the interval  $[-1, 1]$ . We need to repeat the feature twice since the number of features corresponds to the number of qubits in our formulation, and we are not interested in testing single-qubit circuits. Each dataset is then used to define the training, validation, and testing set each one created by randomly subsampling 90 elements out of the original dataset. Thus, the training, validation, and testing datasets partially overlap.

We have also used five real-world regression datasets: the prediction of the price of fish [55], cancer mortality rates in US [56], worldwide life expectancy [57], the cost of medical treatments [58], the cost of the real estate market [59]. The datasets have been preprocessed with PCA to find the 5 principal components. For each dataset, the training, validation, and testing set has been found by subsampling 150 random elements from the whole dataset. Any feature and label have been resized to fit the interval  $[-1, 1]$ . The details of the datasets are shown in Table 1.

Name	Source	License	#F	#PC	#E	#SE
Fish market	[55]	GPL-2	6	5	159	150
OLS cancer	[56]	Public domain	33	5	3047	150
Life Expectancy	[57]	Public domain	31	5	3111	150
Medical Bill	[58]	DbCL v1.0	6	5	1338	150
Real estate	[59]	Public Domain	7	5	414	150
$\sin^2$ function	A	See code	2	2	100	90
Step function	A	See code	2	2	100	90
Meyer Wavelet	A	See code	2	2	100	90

**Table 1:** Dataset specifications. Legend: #F: number of features, #PC: principal components, #E: number of elements of the dataset, #SE: number of sampled elements per training, validation, and testing set, A: artificially generated.

## 4.2 Experimental setup

We have generated quantum kernels using different techniques. We first tried the PQC scheme in Figure 1 by optimizing the circuit using a greedy local search algorithm, simulated annealing, and genetic algorithms. The optimization phase is allowed to estimate both the empirical error of the training set and the generalization error with respect to a validation set. We show the effect of the optimization by comparing the generalization error of the model using the PQC as quantum embedding before and after the optimization. The generalization error in the comparison is calculated with respect to a testing set that is different from the validation one.

We have tested the configuration with  $L = 3$  layers. The matrix for the PQC has been initialized randomly. The greedy algorithm is deterministic and the cost function is queried as many times as the number of gates. The simulated annealing algorithm has been run for 50000 iterations (queries of the cost function) starting with temperature 25000.0 and decreasing exponentially to 2.5. The genetic algorithm has considered an initial population of 50 elements; for each of the 10000 iterations, we select the best 10 instances which are then merged and mutated to generate the next generation of 50 elements. Each iteration discards the old generation. The pseudocode for all optimization techniques is shown in Appendix A.

Then, we have compared our approach with highly expressive PQC in the form:

$$U_{\text{he}}(\theta) = \exp\left(-i \sum_{i \in \{1, \dots, 4^n - 1\}} \theta_i \sigma_i\right) \quad (9)$$

where  $\sigma_i$  are a product of Pauli matrices with  $\sigma_0$  product of identities, and the angles  $\theta_i = x_i w_i$  are obtained by multiplying the feature  $x_i$  with weight  $w_i$  randomly sampled from a normal distribution of mean 0 and variance 1. This kind of circuit has an exponential length in the number of qubits and is the most general scheme for a PQC, with [25] suggesting we shouldn't use it for quantum embedding since its high expressibility will affect the generalization performances. In contrast with all the other approaches having a number of qubits equal to the number of data features, here the number  $n$  is independent of the number of features  $m$ . If  $m < 4^n - 1$  number of parameters, the data features are repeated until any parameter has been assigned.

Finally, we have compared the approaches with randomly generated PQC with an arbitrary number of gates, in the form:

$$U_{\text{rand}}(\theta) = \prod_{\ell=1}^L \left( \prod_{j=1}^{\lceil 0.3n \rceil} \text{CNOT}^{(q_j, q'_j)} \right) \left( \prod_{i=1}^n \exp\left(-ix_i \sigma_{\ell, i}^{(i)}\right) \right) \quad (10)$$

where the  $\text{CNOT} = |0\rangle\langle 0| \otimes \mathbb{I} + |1\rangle\langle 1| \otimes X$  gates are applied to randomly chosen locations  $q_j, q'_j$  and the single qubit rotations are applied to qubit  $i$  and has generator  $\sigma_{\ell, i} \in \{\sigma_x, \sigma_y, \sigma_z\}$ . Each layer has at  $\lceil 0.3n \rceil$  CNOTs. We have tested this scheme with  $L = 3$  layers. The procedure generates a less expressive circuit than  $U_{\text{he}}$  as long as the number of layers is small.

The experiments have been performed on a noiseless, linear algebra-based simulator on the PennyLane framework and JAX simulator. For any circuit except  $U_{\text{he}}$ , the number of qubits matches the number of (PCA) features in Table 1. Each experiment (dataset, approach, optimization technique) has been repeated 10 times.

### 4.3 Results

Figure 3a shows that the optimization process can improve the performance of the machine learning model applied to any dataset. The  $\sin^2$  dataset is the

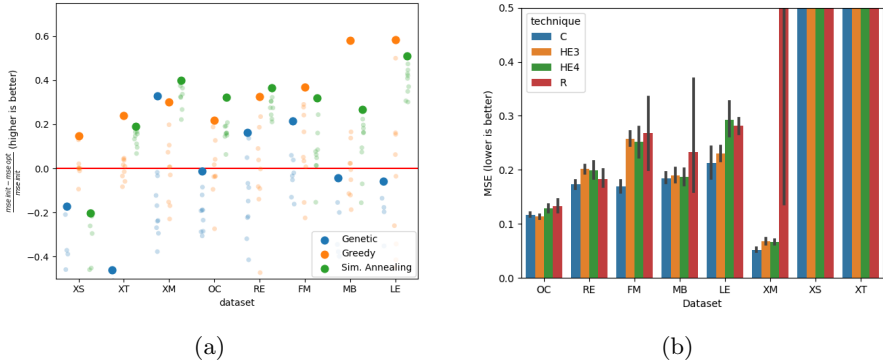


**Fig. 3:** **3a:** effect of the optimization process on the generalization error. On the  $X$ -axis there is the dataset, the  $Y$ -axis is the relative change (ratio between the difference of MSE before and after the process, and the MSE before the process, the maximum value is 1 meaning zero loss after optimization), the hue is the optimization technique. Each semi-transparent point corresponds to a candidate solution, the highlighted point is the best solution found by the optimization technique and all the repetitions of the process, which is the one solution kept. **3b:** comparison of the proposed approaches in terms of MSE. The  $X$ ,  $Y$ -axes and hue have the same meaning; the bar represents the average MSE while the error bars represent the standard deviation. *Dataset legend:* XS:  $\sin^2$  function, XT: step function, XM: Meyer wavelet function, OC: OLC cancer, RE: real estate, FM: fish market, MB: medical bill dataset, LE: life expectancy. *Technique legend:* C: any optimized circuit (include all three techniques), HE3:  $U_{\text{he}}$  acting on three qubits, HE4:  $U_{\text{he}}$  acting on four qubits, R:  $U_{\text{rand}}$ .

one dataset that benefits less from our optimization, although we are able to reduce the 19% the MSE using the greedy local search, while Medical Bill and Life Expectancy datasets benefit the most, both reducing the MSE by the 58% approximately. Table 2 shows the numerical details. We can note that different optimization processes can lead to dramatically different results, with the Genetic algorithm performing worse in general and the deterministic Greedy local search performing best.

Figure 3b shows that our approach has better performances compared to any approach tested, with the improvement varying largely with respect to the dataset. It is important to note that  $U_{\text{he}}$  acting on three-qubits always outperforms  $U_{\text{he}}$  acting on four-qubits. The phenomenon is justified by the spectral properties of the kind of circuit worsen when increasing the number of qubits: according to [25] the largest eigenvalue of the kernel matrix decrease exponentially by increasing the number of qubits, resulting in the impossibility to learn any function.  $U_{\text{rand}}$  is a much simpler circuit than  $U_{\text{he}}$  in terms of the number of gates and we expect to have favorable spectral properties. Although, the simple structure of  $U_{\text{rand}}$  is also the reason for its ineffectiveness. That suggests the solutions found by the optimization process to be a good

compromise, expressible enough to solve the problem but not enough to struggle to generalize.

Detailed results are shown in Appendix D.

## 5 Conclusions

Quantum kernels are a promising technique of quantum machine learning, that in some cases can even lead to an exponential speedup [22]. However, in order to construct effective transformations, their design must be guided by some prior knowledge of the problem. When constructing a quantum embedding such a knowledge is usually lacking. Our proposal is to use optimization algorithms for designing optimal circuits for quantum embedding by heuristically searching the data. We have modeled the problem as a combinatorial optimization problem on gates generators, angles, and positions and formulated it as the minimization of a certain cost function. In contrast with gradient-descent-based approaches [32], which train only the rotational angles of some gates incurring in the barren plateau issue, we avoid this problem by construction. [30] has shown the set of generators of the circuit directly influence the expressibility of the transformation, which leads to the barren plateau [27]: in [32] the generators are fixed and decided a priori, while during our optimization process the generators are varying, and the ineffective (uselessly expressive) solutions are discarded.

The combinatorial optimization process is expensive: the cost function must be queried for any candidate solution. Since the cost function should depend on the generalization error of the model (created using the candidate solution as a circuit), each call of the cost function must create the Gram matrix to be fed to the SVM, which has a quadratic cost in the number of data. We have introduced a policy to discard all the candidate solutions that result in an exponential concentration of kernel similarities around their mean [29], which can be estimated quickly and in constant time, speeding up the process. The candidate solutions whose variance is below the decided threshold are kept and their cost is their generalization error. A higher threshold discards more solutions, speeding up the process as far as needed.

Our experimental results on artificial and real-world datasets have shown that our approach can largely reduce the generalization error, up to 57%. The results depend on the dataset and the optimization process. This suggests that more sophisticated algorithms can further improve performances. We believe that the optimization process can be further improved by exploiting symmetries in quantum transformations to reduce the space of candidate solutions.

## References

- [1] Biamonte, J., Wittek, P., Pancotti, N., Rebentrost, P., Wiebe, N., Lloyd, S.: Quantum machine learning. *Nature* **549**(7671), 195–202 (2017)
- [2] Harrow, A.W., Hassidim, A., Lloyd, S.: Quantum algorithm for linear systems of equations. *Physical review letters* **103**(15), 150502 (2009)

- [3] Rebentrost, P., Mohseni, M., Lloyd, S.: Quantum support vector machine for big data classification. *Physical review letters* **113**(13), 130503 (2014)
- [4] Lloyd, S., Mohseni, M., Rebentrost, P.: Quantum principal component analysis. *Nature Physics* **10**(9), 631–633 (2014)
- [5] Lloyd, S., Garnerone, S., Zanardi, P.: Quantum algorithms for topological and geometric analysis of data. *Nature communications* **7**(1), 1–7 (2016)
- [6] Aaronson, S.: Read the fine print. *Nature Physics* **11**(4), 291–293 (2015)
- [7] Giovannetti, V., Lloyd, S., Maccone, L.: Quantum random access memory. *Physical review letters* **100**(16), 160501 (2008)
- [8] Preskill, J.: Quantum computing in the nisq era and beyond. *Quantum* **2**, 79 (2018)
- [9] Cerezo, M., Arrasmith, A., Babbush, R., Benjamin, S.C., Endo, S., Fujii, K., McClean, J.R., Mitarai, K., Yuan, X., Cincio, L., *et al.*: Variational quantum algorithms. *Nature Reviews Physics* **3**(9), 625–644 (2021)
- [10] Peruzzo, A., McClean, J., Shadbolt, P., Yung, M.-H., Zhou, X.-Q., Love, P.J., Aspuru-Guzik, A., O’Brien, J.L.: A variational eigenvalue solver on a photonic quantum processor. *Nature communications* **5**(1), 1–7 (2014)
- [11] Farhi, E., Goldstone, J., Gutmann, S.: A quantum approximate optimization algorithm. *arXiv preprint arXiv:1411.4028* (2014)
- [12] Zhou, L., Wang, S.-T., Choi, S., Pichler, H., Lukin, M.D.: Quantum approximate optimization algorithm: Performance, mechanism, and implementation on near-term devices. *Physical Review X* **10**(2), 021067 (2020)
- [13] Abbas, A., Sutter, D., Zoufal, C., Lucchi, A., Figalli, A., Woerner, S.: The power of quantum neural networks. *Nature Computational Science* **1**(6), 403–409 (2021)
- [14] Havlíček, V., Córcoles, A.D., Temme, K., Harrow, A.W., Kandala, A., Chow, J.M., Gambetta, J.M.: Supervised learning with quantum-enhanced feature spaces. *Nature* **567**(7747), 209–212 (2019)
- [15] Shawe-Taylor, J., Cristianini, N.: *Kernel Methods for Pattern Analysis*. Cambridge University Press, Cambridge, UK (2004)
- [16] Hofmann, T., Schölkopf, B., Smola, A.J.: Kernel methods in machine learning. *The annals of statistics* **36**(3), 1171–1220 (2008)
- [17] Schölkopf, B., Tsuda, K., Vert, J.-P.: *Kernel Methods in Computational Biology*. MIT press, Cambridge, MA (2004)

- [18] Ralaivola, L., Swamidass, S.J., Saigo, H., Baldi, P.: Graph kernels for chemical informatics. *Neural networks* **18**(8), 1093–1110 (2005)
- [19] Karniadakis, G.E., Kevrekidis, I.G., Lu, L., Perdikaris, P., Wang, S., Yang, L.: Physics-informed machine learning. *Nature Reviews Physics* **3**(6), 422–440 (2021)
- [20] Schuld, M.: Supervised quantum machine learning models are kernel methods. arXiv preprint arXiv:2101.11020 (2021)
- [21] Gottesman, D., Chuang, I.: Quantum digital signatures. arXiv preprint quant-ph/0105032 (2001)
- [22] Liu, Y., Arunachalam, S., Temme, K.: A rigorous and robust quantum speed-up in supervised machine learning. *Nature Physics* **17**(9), 1013–1017 (2021)
- [23] Glick, J.R., Gujarati, T.P., Corcoles, A.D., Kim, Y., Kandala, A., Gambetta, J.M., Temme, K.: Covariant quantum kernels for data with group structure. arXiv preprint arXiv:2105.03406 (2021)
- [24] Huang, H.-Y., Broughton, M., Mohseni, M., Babbush, R., Boixo, S., Neven, H., McClean, J.R.: Power of data in quantum machine learning. *Nature Communications* **12**(1) (2021). <https://doi.org/10.1038/s41467-021-22539-9>
- [25] Kübler, J., Buchholz, S., Schölkopf, B.: The inductive bias of quantum kernels. *Advances in Neural Information Processing Systems* **34** (2021)
- [26] Canatar, A., Peters, E., Pehlevan, C., Wild, S.M., Shaydulin, R.: Bandwidth enables generalization in quantum kernel models. arXiv preprint arXiv:2206.06686 (2022)
- [27] Holmes, Z., Sharma, K., Cerezo, M., Coles, P.J.: Connecting ansatz expressibility to gradient magnitudes and barren plateaus. *PRX Quantum* **3**(1), 010313 (2022)
- [28] McClean, J.R., Boixo, S., Smelyanskiy, V.N., Babbush, R., Neven, H.: Barren plateaus in quantum neural network training landscapes. *Nature communications* **9**(1), 1–6 (2018)
- [29] Thanasilp, S., Wang, S., Cerezo, M., Holmes, Z.: Exponential concentration and untrainability in quantum kernel methods. arXiv preprint arXiv:2208.11060 (2022)
- [30] Larocca, M., Czarnik, P., Sharma, K., Muraleedharan, G., Coles, P.J., Cerezo, M.: Diagnosing barren plateaus with tools from quantum optimal control. arXiv preprint arXiv:2105.14377 (2021)

- [31] Mitarai, K., Negoro, M., Kitagawa, M., Fujii, K.: Quantum circuit learning. *Physical Review A* **98**(3), 032309 (2018)
- [32] Lloyd, S., Schuld, M., Ijaz, A., Izaac, J., Killoran, N.: Quantum embeddings for machine learning. arXiv preprint arXiv:2001.03622 (2020)
- [33] Altares-López, S., Ribeiro, A., García-Ripoll, J.J.: Automatic design of quantum feature maps. *Quantum Science and Technology* **6**(4), 045015 (2021)
- [34] Chen, B.-S., Chern, J.-L.: Genetically auto-generated quantum feature maps. arXiv preprint arXiv:2207.11449 (2022)
- [35] Huang, Y., Li, Q., Hou, X., Wu, R., Yung, M.-H., Bayat, A., Wang, X.: Robust resource-efficient quantum variational ansatz through an evolutionary algorithm. *Physical Review A* **105**(5), 052414 (2022)
- [36] Murphy, K.P.: *Machine Learning: a Probabilistic Perspective*. MIT press, Cambridge, MA (2012)
- [37] Cortes, C., Vapnik, V.: Support-vector networks. *Machine learning* **20**(3), 273–297 (1995)
- [38] Schölkopf, B., Smola, A., Müller, K.-R.: Nonlinear component analysis as a kernel eigenvalue problem. *Neural computation* **10**(5), 1299–1319 (1998)
- [39] Caponnetto, A., De Vito, E.: Optimal rates for the regularized least-squares algorithm. *Foundations of Computational Mathematics* **7**(3), 331–368 (2007)
- [40] Amini, A.A., Razaee, Z.S.: Concentration of kernel matrices with application to kernel spectral clustering. *The Annals of Statistics* **49**(1), 531–556 (2021)
- [41] Cristianini, N., Shawe-Taylor, J., Elisseeff, A., Kandola, J.: On kernel-target alignment. *Advances in neural information processing systems* **14** (2001)
- [42] Cortes, C., Mohri, M., Rostamizadeh, A.: Algorithms for learning kernels based on centered alignment. *The Journal of Machine Learning Research* **13**, 795–828 (2012)
- [43] Sim, S., Johnson, P.D., Aspuru-Guzik, A.: Expressibility and entangling capability of parameterized quantum circuits for hybrid quantum-classical algorithms. *Advanced Quantum Technologies* **2**(12), 1900070 (2019)
- [44] Nakaji, K., Yamamoto, N.: Expressibility of the alternating layered ansatz for quantum computation. *Quantum* **5**, 434 (2021)

- [45] Cerezo, M., Sone, A., Volkoff, T., Cincio, L., Coles, P.J.: Cost function dependent barren plateaus in shallow parametrized quantum circuits. *Nature communications* **12**(1), 1–12 (2021)
- [46] Wang, S., Fontana, E., Cerezo, M., Sharma, K., Sone, A., Cincio, L., Coles, P.J.: Noise-induced barren plateaus in variational quantum algorithms. *Nature communications* **12**(1), 1–11 (2021)
- [47] Albertini, F., D’Alessandro, D.: Notions of controllability for bilinear multilevel quantum systems. *IEEE Transactions on Automatic Control* **48**(8), 1399–1403 (2003)
- [48] Larocca, M., Ju, N., García-Martín, D., Coles, P.J., Cerezo, M.: Theory of overparametrization in quantum neural networks. *arXiv preprint arXiv:2109.11676* (2021)
- [49] Kirkpatrick, S., Gelatt Jr, C.D., Vecchi, M.P.: Optimization by simulated annealing. *science* **220**(4598), 671–680 (1983)
- [50] Katoch, S., Chauhan, S.S., Kumar, V.: A review on genetic algorithm: past, present, and future. *Multimedia Tools and Applications* **80**(5), 8091–8126 (2021)
- [51] Cvijović, D., Klinowski, J.: Taboo search: an approach to the multiple minima problem. *Science* **267**(5198), 664–666 (1995)
- [52] Schuetz, M.J., Brubaker, J.K., Katzgraber, H.G.: Combinatorial optimization with physics-inspired graph neural networks. *Nature Machine Intelligence* **4**(4), 367–377 (2022)
- [53] Mazyavkina, N., Sviridov, S., Ivanov, S., Burnaev, E.: Reinforcement learning for combinatorial optimization: A survey. *Computers & Operations Research* **134**, 105400 (2021)
- [54] Daubechies, I.: *Ten Lectures on Wavelets*. SIAM, Philadelphia, PE (1992)
- [55] Pyae, A.: Fish Market (dataset). Kaggle (2019). <https://www.kaggle.com/datasets/aungpyaeap/fish-market>
- [56] Rippner, N.: OLS Regression Challenge (dataset). Kaggle (2019). <https://data.world/rippner/ols-regression-challenge>
- [57] Rajarshi, K.: Life Expectancy (dataset). Kaggle (2016). <https://www.kaggle.com/datasets/kumarajarshi/life-expectancy-who>
- [58] Stednick, Z.: Medical Cost Personal (dataset). Kaggle (2017). <https://www.kaggle.com/datasets/mirichoi0218/insurance>
- [59] Algor\_Bruce: Real Estate. Kaggle (2021). <https://www.kaggle.com/>

[datasets/quantbruce/real-estate-price-prediction](#)

- [60] Lukac, M., Perkowski, M., Goi, H., Pivtoraiko, M., Yu, C.H., Chung, K., Jeech, H., Kim, B.-G., Kim, Y.-D.: Evolutionary approach to quantum and reversible circuits synthesis. *Artificial Intelligence Review* **20**(3), 361–417 (2003). <https://doi.org/10.1023/B:AIRE.0000006605.86111.79>
- [61] Di Marcantonio, F., Incudini, M., Tezza, D., Grossi, M.: Quask–quantum advantage seeker with kernels. *arXiv preprint arXiv:2206.15284* (2022)
- [62] Bergholm, V., Izaac, J., Schuld, M., Gogolin, C., Alam, M.S., Ahmed, S., Arrazola, J.M., Blank, C., Delgado, A., Jahangiri, S., et al.: Pennylane: Automatic differentiation of hybrid quantum-classical computations. *arXiv preprint arXiv:1811.04968* (2018)
- [63] Bradbury, J., Frostig, R., Hawkins, P., Johnson, M.J., Leary, C., Maclaurin, D., Necula, G., Paszke, A., VanderPlas, J., Wanderman-Milne, S., Zhang, Q.: JAX: Composable Transformations of Python+NumPy programs. <http://github.com/google/jax>

## A Pseudocode for Meta-Heuristic optimization algorithms

Figure 4 shows the pseudocode of the greedy algorithm that we have used to optimize the PQC. Starting from an initial configuration scheme representing our candidate solution, the algorithm mutates a single operation while keeping fixed the others. Each possible combination of generators and features for the single operation are tested, and the best one (in terms of cost function query) is kept. The procedure is repeated for any gate of the circuit, thus  $2nL$  times for the rigid structure in Figure 1.

Figure 5 shows the pseudocode of the genetic algorithm employed in our experiments. Genetic algorithms [50] are probabilistic meta-heuristic optimization techniques inspired by natural selection. An initial population of candidate solutions called *chromosome* is randomly generated. Each chromosome is usually represented as a vector or matrix of integer elements. In our case, it is represented by the matrix in Figure 1. The components of the chromosomes are the genes. We evolve the population through an arbitrary number of iterations, the population of each iteration is a *generation*. Each element of the population has a fitness value, which corresponds to an inverse cost (the higher the fitness, the better the solution). Each iteration is composed of the *selection* step, the *crossover* step and the *mutation* step. The selection step chooses a subset of the population to be bred and generate children. We select the 20% best items of the population to be bred, but several other policies can be used. The selected items are then used to instantiate the new generation during the crossover phase: each child is generated using the first  $m$  columns of the left parent, and the other columns from the right parent, with  $m$  chosen randomly each time. Other crossover policies are allowed. Finally, each child is

```

Data: initial circuit matrix  $M$  of size  $2 \times 2Ln$ , data point
         $x$ , cost function  $C(M)$ 
Result: final circuit matrix  $M$  of size  $2 \times 2Ln$ 
 $P \leftarrow \{\mathbb{I}_2, \sigma_x, \sigma_y, \sigma_z\}$ ;
best_cost  $\leftarrow +\infty$ ;
for  $\ell \in \{0, \dots, L\}$  do
    for  $i \in \{0, \dots, 2n\}$  do
         $\triangleright$  For each layer  $\ell$ 
        for  $i \in \{0, \dots, 2n\}$  do
             $\triangleright$  For each gate in the layer
            if  $i < n$  then
                 $\triangleright$  Single-qubit gate
                for  $p \in P$  do
                     $\triangleright$  Assign a generator
                     $M' \leftarrow M$ ;
                     $M'[2\ell n + i][0] \leftarrow p$ ;
                    for  $j \in \{0, \dots, n\}$  do
                         $\triangleright$  Assign an angle
                         $M'[2\ell n + i][1] \leftarrow x_j$ ;
                        if  $C(M') < \text{best\_cost}$  then
                             $M \leftarrow M'$ 
                        end
                    end
                end
            else
                 $\triangleright$  2-local gate
                for  $p \in P \otimes P$  do
                     $\triangleright$  Assign a generator
                     $M' \leftarrow M$ ;
                     $M'[2\ell n + i][0] \leftarrow p$ ;
                    for  $j \in \{0, \dots, n\}$  do
                         $\triangleright$  Assign an angle
                         $M'[2\ell n + i][1] \leftarrow x_j$ ;
                        if  $C(M') < \text{best\_cost}$  then
                             $M \leftarrow M'$ 
                        end
                    end
                end
            end
        end
    end
end
return  $M$ 
    
```

**Fig. 4:** Pseudocode for the Greedy Local Search

then mutated by perturbing one or more genes (e.g. adding 1 to the gene). The new generation substitutes completely the old one, although the algorithm can be tuned to have only a small part of the population be substituted. Genetic algorithms have been extensively investigated in the context of quantum circuit synthesis with satisfactory results [60].

Figure 6 shows the pseudocode of the Simulated Annealing algorithm [49]. Simulated Annealing is a probabilistic meta-heuristic optimization techniques inspired by the annealing process in metallurgy. An initial set of candidate solution is randomly generated at the beginning of the process. For each solution, the annealing process perform an arbitrary number of iterations that perturbs the candidate solution. If the perturbed solution has lower cost than the original one, the former is accepted as new candidate solution in substitution of the latter. If the perturbed solution has higher cost, it can be either accepted or rejected through a probabilistic policy that depends on both the difference of energy and a temperature parameter  $T$ : low energy differences and high temperature results in higher chances of solution acceptance. The temperature parameter decreases linearly or exponentially toward a minimum value ( $T_{\min} \geq 0$ ) at each iteration. The varying of temperature allow to explore the space of solution at the beginning of the process, while at the end of the

```

Data:
    population pop (list) of initial circuit matrices M of size  $2 \times 2Ln$ 
    (the first row of each matrix contains the integers identifying
    the generators, the second row contains
    the indexes of the features representing the rotation angles),
    fitness function  $F(M)$ ,
    max iteration I,
    number of parents mating B.

Result:
    final population of circuit matrices M of size  $2 \times 2Ln$ ,
    best matrix  $M_{best}$  in the final population.

P  $\leftarrow [\mathbb{I}_2, \sigma_x, \sigma_y, \sigma_z]$ ; ▷ Base set of generators

for i  $\in [0, \dots, I]$  do ▷ For each iteration i
    newPop  $\leftarrow []$ ;
    fitnessList  $\leftarrow []$ ;
    parents  $\leftarrow$  select B random matrices from pop; ▷ Compute Fitness

    for M  $\in$  pop do
        f  $\leftarrow F(M)$ ;
        fitnessList  $\leftarrow f$ ; ▷ Keep the B matrices with higher fitness
        if f is in the top B of fitnessList then
            remove matrix with lower fitness from parents;
            parents.APPEND(M);
        end
    newPop  $\leftarrow$  parents; ▷ For each missing matrix in the offspring

    for m  $\in [0, \dots, \text{len}(\text{pop}) - B]$  do ▷ Perform crossover
        p1, p2  $\leftarrow$  select 2 random matrices from parents;
        split  $\leftarrow$  RANDOMINT(0,  $2Ln$ ); ▷ Split and concatenate parent matrices
        leftside  $\leftarrow p1[:, 0 : \text{split}]$ ;
        rightside  $\leftarrow p2[:, \text{split} : 2Ln]$ ;
        children  $\leftarrow$  CONCATENATE(leftside, rightside); ▷ For each gene

        for gene  $\in [0, \dots, 2Ln]$  do ▷ Perform mutation with a probability of 10%
            prob  $\leftarrow$  RANDOMUNIFORM();
            if prob  $<$  0.1 then ▷ Randomly chose generator and angle
                generator  $\leftarrow$  RANDOMINT(0,  $\text{len}(P \otimes P)$ );
                angle  $\leftarrow$  RANDOMINT(0, n); ▷ Assign new generator and angle
                children[0][gene]  $\leftarrow$  generator;
                children[1][gene]  $\leftarrow$  angle;
            end
        newPop.APPEND(children)
    end ▷ Update population with the new one

    pop  $\leftarrow$  newPop
end
return pop

```

**Fig. 5:** Pseudocode for the Genetic algorithm

process we converge to a local or global minima. At the end of the process, we have a number of optimized solutions matching the initial candidate solutions. The best solution in this set is kept.

## B Pseudocode for circuit construction

The code for constructing  $U_{he}$  is taken from PennyLane framework. It corresponds to the pseudocode shown in Figure 7a. The code for constructing  $U_{rand}$

```

Data:
initial circuit matrix  $M$  of size  $2 \times 2Ln$ : the first row contains
the integers identifying the generators, the second row contains
the indexes of the features representing the rotation angles,
energy function  $E(M)$ ,
max iteration  $I$ .
Result:
best matrix  $M_{best}$  of size  $2 \times 2Ln$ .

 $P \leftarrow [\mathbb{I}_2, \sigma_x, \sigma_y, \sigma_z]$ ;
 $T_{max} \leftarrow 25000$ ,  $T_{min} \leftarrow 2.5$ ;
 $T_f \leftarrow -\log(T_{max}/T_{min})$ ;
                                 $\triangleright$  Initial state initialization

 $M_{old} \leftarrow M$ ;
 $energy \leftarrow E(M)$ ;
 $energy_{old} \leftarrow energy$ ;
                                 $\triangleright$  Best state initialization

 $M_{best} \leftarrow M$ ;
 $energy_{best} \leftarrow energy$ ;
                                 $\triangleright$  For each iteration  $i$ 
for  $i \in [0, \dots, I]$  do
                                 $\triangleright$  Update temperature
     $T \leftarrow T_{max} \exp\{iT_f/I\}$ ;
                                 $\triangleright$  Change state
     $index \leftarrow \text{RANDOMINT}(0, 2Ln)$ ;
    if  $probab < \text{RANDOMUNIFORM}(0, 1)$  then
                                 $\triangleright$  Change generator
         $M[0][index] \leftarrow (M[0][index] + 1) \% \text{len}(P \otimes P)$ ;
    else
                                 $\triangleright$  Change angle
         $M[1][index] \leftarrow (M[1][index] + 1) \% n$ ;
    end
     $energy \leftarrow E(M)$ ;
     $\Delta E \leftarrow energy - energy_{old}$ ;
     $\triangleright$  Decide whether to accept the new state depending on
    temperature and energy
    if  $\Delta E < 0$  and  $\exp\{-\Delta E/T\} < \text{RANDOMUNIFORM}(0, 1)$  then
                                 $\triangleright$  Restore previous state
         $M \leftarrow M_{old}$ ;
         $energy \leftarrow energy_{old}$ ;
    else
                                 $\triangleright$  Accept new state
         $M_{old} \leftarrow M$ ;
         $energy_{old} \leftarrow energy$ ;
        if  $energy_{best} < energy$  then
                                 $\triangleright$  Store best solution
             $M_{best} \leftarrow M$ ;
             $energy_{best} \leftarrow energy$ ;
        end
    end
end
return  $M_{best}$ 

```

**Fig. 6:** Pseudocode for Simulated Annealing algorithm

is shown in Figure 7b. The code for constructing the scheme of PQC having the fixed structure in Figure 1 is shown in Figure 7c.

## C Code and implementation details

The software for the experiments has been developed using Quask [61], which is a software running on top of PennyLane [62] framework. The noiseless, linear algebra-based simulator is based on the JAX library [63] which allows for faster simulations of quantum circuits. The code to reproduce the experiments, including intermediate results and plot can be freely downloaded from <https://github.com/incud/Combinatorial-Optimization-Quantum-Embeddings>.

```

Data:  $n$  number of qubits of the quantum embedding.  $w$  a
vector of random weights having  $4^n - 1$  components
sampled from a zero-mean normal distribution of
variance 1.  $x$  a data point having  $m$  features.
Result: The circuit for the quantum embedding.
 $x \leftarrow$  repeat  $x$  components until size  $4^n - 1$  is reached
for each  $n$ -qubits product of Pauli matrices  $p$  (index  $k$ ) do
  if  $p$  is product of only identities then
    continue
  end
   $m \leftarrow$  list of active qubits (non-identity)
   $\triangleright$  Rotate to prepare for Multi-Z
  for wire  $i = 0, \dots, \text{len}(m)$  do
    if  $p[m[i]] = \sigma_x$  then
      Apply  $H$  on wire  $i$ 
    else if  $p[m[i]] = \sigma_y$  then
      Apply  $\exp(-i\frac{\pi}{2}\sigma_x)$  on wire  $i$ 
    end
  end
   $\triangleright$  Multi-Z gate
  for wire  $i = \text{len}(m), \dots, 1$  do
    Apply  $CNOT$  on  $m[i], m[i] - 1$  qubits
  end
  Apply  $\exp(-ix_k w_k \sigma_x)$  on  $m[0]$ 
  for wire  $i = 0, \dots, \text{len}(m)$  do
    Apply  $CNOT$  on  $m[i], m[i] + 1$  qubits
  end
   $\triangleright$  Reverse previous rotations
  for wire  $i = 0, \dots, \text{len}(m)$  do
    if  $p[m[i]] = \sigma_x$  then
      Apply  $H$  on wire  $i$ 
    else if  $p[m[i]] = \sigma_y$  then
      Apply  $\exp(-i\frac{\pi}{2}\sigma_x)$  on wire  $i$ 
    end
  end
end

```

(a)

```

Data:  $n$  number of qubits of the quantum embedding.  $w$  a
vector of random weights having  $4^n - 1$  components
sampled from a zero-mean normal distribution of
variance 1.  $x$  a data point having  $m$  features.
Result: The circuit for the quantum embedding.
 $x \leftarrow$  repeat  $x$  components until size  $4^n - 1$  is reached
for each  $n$ -qubits product of Pauli matrices  $p$  (index  $k$ ) do
  if  $p$  is product of only identities then
    continue
  end
   $m \leftarrow$  list of active qubits (non-identity)
   $\triangleright$  Rotate to prepare for Multi-Z
  for wire  $i = 0, \dots, \text{len}(m)$  do
    if  $p[m[i]] = \sigma_x$  then
      Apply  $H$  on wire  $i$ 
    else if  $p[m[i]] = \sigma_y$  then
      Apply  $\exp(-i\frac{\pi}{2}\sigma_x)$  on wire  $i$ 
    end
  end
   $\triangleright$  Multi-Z gate
  for wire  $i = \text{len}(m), \dots, 1$  do
    Apply  $CNOT$  on  $m[i], m[i] - 1$  qubits
  end
  Apply  $\exp(-ix_k w_k \sigma_x)$  on  $m[0]$ 
  for wire  $i = 0, \dots, \text{len}(m)$  do
    Apply  $CNOT$  on  $m[i], m[i] + 1$  qubits
  end
   $\triangleright$  Reverse previous rotations
  for wire  $i = 0, \dots, \text{len}(m)$  do
    if  $p[m[i]] = \sigma_x$  then
      Apply  $H$  on wire  $i$ 
    else if  $p[m[i]] = \sigma_y$  then
      Apply  $\exp(-i\frac{\pi}{2}\sigma_x)$  on wire  $i$ 
    end
  end
end

```

(b)

```

Data:  $M$  matrix of  $2 \times 2Ln$  components.  $x$  a data point
having  $n$  features.
Result: The circuit for the quantum embedding.  $|P\rangle = 4$ 
 $P \leftarrow [x_2, \sigma_x, \sigma_y, \sigma_x]$ 
 $P_2 \leftarrow P \otimes P$   $\triangleright$  Pairwise tensor product,  $|P_2\rangle = 16$ 
for layer  $\ell \in 1, \dots, L$  do
   $\triangleright$  Single qubit operation
  for  $i \in 0, \dots, n$  do
    generator  $\leftarrow M[\ell][2n\ell + i]$ 
    feature  $\leftarrow M[\ell][2n\ell + i]$ 
     $\sigma \leftarrow P[\text{generator}]$ 
     $\theta \leftarrow x[\text{feature}]$ 
    Apply  $\exp(-i\theta\sigma)$  on qubit  $i$ 
  end
   $\triangleright$  Two qubits operation
  for  $i \in 0, \dots, n$  do
    generator  $\leftarrow M[\ell][2n\ell + n + i]$ 
    feature  $\leftarrow M[\ell][2n\ell + n + i]$ 
     $\sigma \leftarrow P_2[\text{generator}]$ 
     $\theta \leftarrow x[\text{feature}]$ 
    Apply  $\exp(-i\theta\sigma)$  on qubits  $i, (i+1) \bmod n$ 
  end
end

```

(c)

**Fig. 7:** 7a: pseudocode for construct the circuit corresponding to  $U_{\text{he}}$  unitary transformation. 7b: pseudocode for construct the circuit corresponding to  $U_{\text{rand}}$  unitary transformation. 7c: pseudocode for construct the circuit corresponding to the fixed scheme of PQC in Figure 1.

## D Detailed results

In Table 2 we show the change of MSE before and after the optimization process for each technique. Figure 8 shows the detailed MSE for any dataset and kernel technique proposed.

Dataset	Optimization technique	$\frac{\Delta \text{MSE}}{\text{MSE before opt.}}$	MSE before opt.	MSE after opt.
FM	Genetic	0.2148	0.1739	0.2328
	Greedy	0.3676	0.2150	0.1731
	Sim. Annealing	0.3189	0.2150	0.2123
LE	Genetic	-0.0592	0.2185	0.4565
	Greedy	0.5843	0.3024	0.2943
	Sim. Annealing	0.5097	0.3241	0.2265
MB	Genetic	-0.0415	0.1536	0.2837
	Greedy	0.5798	0.4207	0.2098
	Sim. Annealing	0.2660	0.1996	0.2307
OC	Genetic	-0.0133	0.1072	0.1381
	Greedy	0.2184	0.1429	0.1291
	Sim. Annealing	0.3233	0.1393	0.1304
RE	Genetic	0.1638	0.1686	0.1979
	Greedy	0.3258	0.2809	0.2269
	Sim. Annealing	0.3661	0.2271	0.1792
XM	Genetic	0.3287	0.0602	0.0736
	Greedy	0.2999	0.0600	0.0586
	Sim. Annealing	0.3983	0.0714	0.0556
XS	Genetic	-0.1708	0.5253	1.0796
	Greedy	0.1475	1.0678	1.0678
	Sim. Annealing	-0.2028	0.5869	1.0176
XT	Genetic	-0.4621	1.0537	1.8781
	Greedy	0.2398	1.7907	1.7907
	Sim. Annealing	0.1913	1.9618	1.8295

**Table 2:** Change of performance in terms of MSE before and after the optimization process. These correspond to the best MSE obtained before the optimization among all the repetitions and the best MSE after the optimization among all repetitions, for each dataset. *Dataset legend:* XS:  $\sin^2$  function, XT: step function, XM: Meyer wavelet function, OC: OLC cancer, RE: real estate, FM: fish market, MB: medical bill dataset, LE: life expectancy.

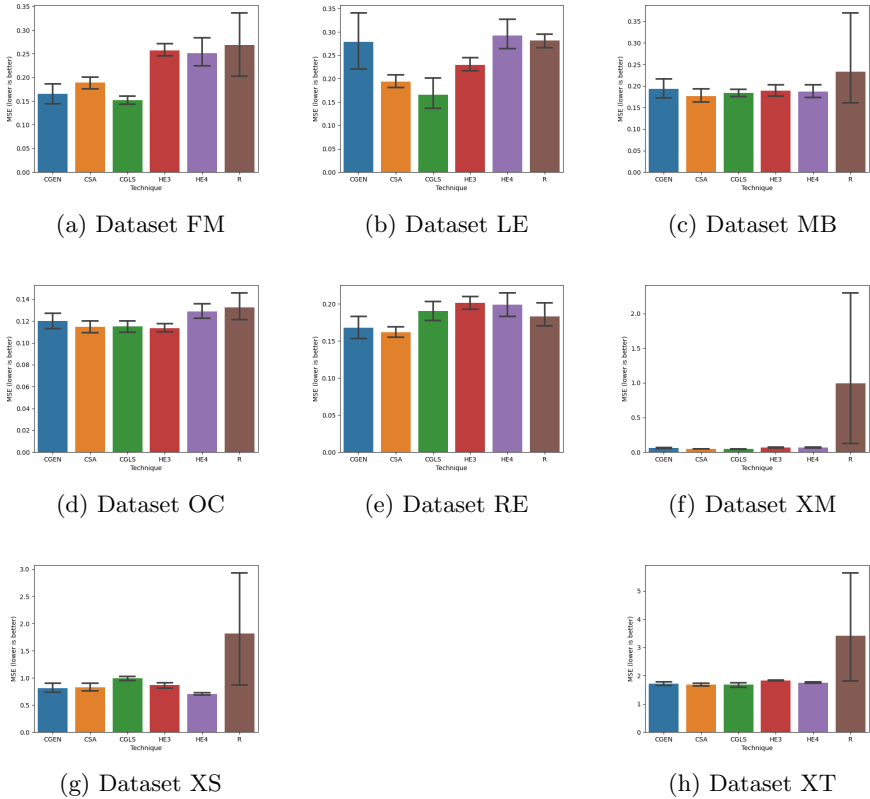


**Fig. 8:** Detailed MSE analysis for any dataset and kernel technique. *Dataset legend:* XS:  $\sin^2$  function, XT: step function, XM: Meyer wavelet function, OC: OLC cancer, RE: real estate, FM: fish market, MB: medical bill dataset, LE: life expectancy. *Technique legend:* CGEN: genetic algorithm optimization approach, GSA: simulated annealing optimized approach, CGLS: greedy local search optimized approach, HE3:  $U_{\text{he}}$  acting on three qubits, HE4:  $U_{\text{he}}$  acting on four qubits, R:  $U_{\text{rand}}$ .